Kinetics and Mechanisms of Thermal Imidization Studies by UV-Visible and Fluorescence Spectroscopic Techniques

Paul R. Dickinson† and Chong Sook Paik Sung*

Institute of Materials Science, Department of Chemistry, University of Connecticut, 97 North Eagleville Road, Storrs, Connecticut 06269-3136

Received November 11, 1991; Revised Manuscript Received February 24, 1992

ABSTRACT: Kinetics and mechanisms of thermal imidization in solution and solid state were studied by UV-visible, fluorescence, FTIR, and size-exclusion chromatography, using polyamic acid synthesized from 1,5-diaminonaphthalene (DAN) and a partially fluorinated dianhydride (6FDA). Since all other reaction intermediates have negligible fluorescence, fluorescence spectroscopy was used to measure the concentration of DAN due to depolymerization from poly(amic acid), which was confirmed by size-exclusion chromatography. Deconvolution of UV-visible spectra using model compound spectra provided compositional analysis of involved species from which the rate constants were extracted. In dilute solution imidization, the depolymerization rate was ~3 times greater than that of imidization, with activation energies of approximately 15 kcal/mol. In a thin film imidized between 150 and 180 °C, much less depolymerization was observed, with the imidization rate slightly faster and activation energy greater than the corresponding parameters in dilute solution. FTIR results provided independent confirmation of the compositional analysis estimated by UV-visible spectral deconvolution.

Introduction

Thermal imidization is the most often used method to obtain polyimides from polyamic acids. During thermal imidization, side reactions other than imidization are known to occur. In order to characterize the kinetics and mechanisms of thermal imidization, it is necessary to identify the other intermediate products involved. In the preceding paper, we described the synthesis of these intermediates and their characterization by UV-visible and fluorescence spectroscopic techniques, using 1,5-diaminonaphthalene (DAN) as a model diamine and phthalic anhydride. In this study, we attempt to comprehensively characterize and analyze the imidization and depolymerization reactions occurring both in dilute solution and in solid films, by using UV-visible and fluorescence results obtained from model compounds. The advantage of the UV-visible technique lies in the fact that it can differentiate between the multitude of reaction species.[1a] The ability to quantify each intermediate by spectral deconvolution would provide information not only on the general kinetics but also on the possible magnitude of substituent effects involved with conjugated monomers. As described in the preceding paper, only DAN is strongly fluorescent while all the other reaction intermediates have negligible fluorescence. Therefore, fluorescence during imidization has been used for a sensitive estimate of depolymerized DAN.

In this study, a partially fluorinated dianhydride (2,2-bis(3,4-dicarboxyphenyl)hexafluoropropane dianhydride, 6FDA) was used with DAN to form polyamic acid. In Scheme I, the R′ group is $C(CF_3)_2$ in 6FDA. In addition to enhancing the solubility of polyimides, 6FDA contains a central conjugation blocking functional group, reducing the maximum wavelength of absorption to approximately that of phthalic anhydride. Therefore, we are justified in using UV-visible spectra obtained from model compounds derived from the reaction of DAN and phthalic anhydride for poly(amic acid) made from DAN and 6FDA. Another reason for the choice of a nonconjugated dianhydride such as 6FDA was to avoid the charge-transfer complexes that

Scheme I
Polyimide Synthesis Considering Depolymerization and Substituent Effects

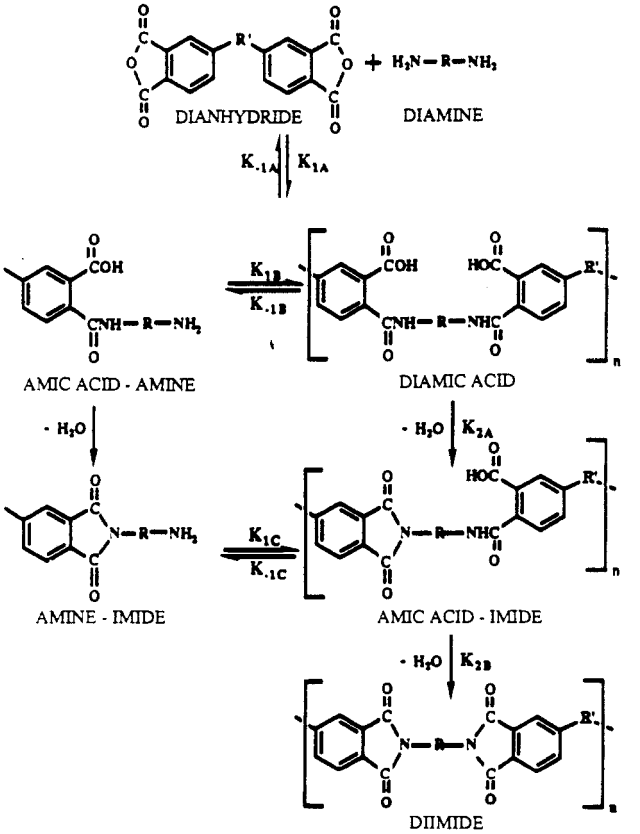

are known to form when both monomers are conjugated.[2] Intensely colored charge-transfer complexes can often interfere with UV-visible spectral analysis.

Experimental Section

Materials. 1,5-Diaminonaphthalene (DAN) was purchased from Fluka Chemical and sublimed twice prior to use. The partially fluorinated dianhydride was electronic grade 2,2-bis-(3,4-dicarboxyphenyl)hexafluoropropane dianhydride (6FDA) from Hoechst Celanese, which was used without further purification. Gold label aniline was from Aldrich Chemical, and polystyrene standards were from Waters Associates. Spectro-

† Present address: AT&T Bell Laboratories, 2000 NE Expressway, Norcross, GA 30071.

0024-9297/92/2225-3758$03.00/0

photometric grade *N*-methylpyrrolidone (NMP) from Aldrich was dried over 4-Å molecular sieves, vacuum distilled over P_2O_5, stored over 4-Å sieves, and filtered with a Teflon filter (0.45-μm pore size) prior to use. Liquid chromatography grade tetrahydrofuran was purchased from EM Science and used without further purification.

Instrumentation. UV–visible and fluorescence spectra were obtained using Perkin-Elmer Lamda Array 3840 UV–visible and Perkin-Elmer MPF-66 fluorescence spectrophotometers, respectively. Size-exclusion chromatography results were obtained via Waters GPC Model 510 equipped with Waters 410 differential refractometer and Waters 484 tunable absorbance detectors. Waters Ultrastyragel columns of 10^4-, 10^3-, 500-, and two 100-Å columns were used in series with tetrahydrofuran as mobile phase at ambient temperatures. FTIR spectra were obtained on a Nicolet 60 SX FTIR using a Wilmad sampling cell containing NaCl plates and a 0.1-mm-thick Teflon spacer.

Reaction Conditions. Poly(amic acid) for solution imidization reactions was synthesized by slow addition of 1.770 g (4.0 mmol) of 6FDA to a solution comprising 0.630 g (4.0 mmol) of DAN in 30 mL of NMP with subsequent stirring at 23 °C for 3 h. For each reaction, 3 mL of the prepared solution was pipeted into 20 mL of NMP to yield a 1.0 wt % solution. The solution imidization was carried out in a 50-mL three-necked flask equipped with a drying tube and preheated argon purged at a rate of 18.5 ± 2 mL/min.

Poly(amic acid) solutions of greater concentration for solid film reactions were prepared by using 21.5 mmol of DAN and 6FDA in 50 mL of NMP. A Gardner knife was used to spread a 15-mil-thick viscous solution of about 10 by 8 in. dimensions on soda lime glass. The films were partially dried for 24 h in a room temperature oven equipped with argon flow, followed by heating at 50 °C in a vacuum oven for an additional 24 h. The films were imidized on the glass substrates, and the samples were acquired by removing ~$^1/_2$-in. strips sequentially from the edge of the film.

The soluble diimide model compound used for IR standard was synthesized from 6FDA and aniline, via imidization at 170 °C in NMP followed by precipitation in water and washing several times with cold water. The product was dried at 50 °C under vacuum for 24 h and used without further purification. Purity estimates from IR spectra exceed 95%.

Reaction Monitoring. UV–Visible Spectroscopy. For the solution reactions, 10-μL aliquots taken from the reaction flask through a rubber septum were diluted into 3 mL of NMP in a cuvette before acquiring a spectrum. For the solid-state reactions, small pieces of the films were dissolved in NMP until a constant absorbance was obtained, which ranged from 0.8 to 1.2.

Fluorescence Spectroscopy. For the solution reactions, 0.8-μL aliquots of sample solution were diluted into 3 mL of NMP in a fluorescence cuvette. The absorbance of this solution did not exceed 0.1 absorbance units. The excitation wavelength was set at 340 nm with the excitation slit and emission slit at 1.0 and 3.0 nm, respectively.

Size-Exclusion Chromatography. For the solution reactions, 100-μL aliquots were injected into the SEC after cooling and filtering through a 0.45-μm pore size filter. For solid-state reactions, pieces of the solid films were dissolved in NMP before injection into SEC. A dilute-solution viscosity experiment confirmed that a polyelectrolyte effect did not exist for this particular system in tetrahydrofuran.

Infrared Spectroscopy. For the solution reactions, a flow cell was used and its path length was controlled by a Teflon spacer such that the absorbance of required peaks did not exceed 0.9 in order to subtract the solvent and obtain quantitative data. Approximately 2-mL aliquots were taken drom the reaction flask before injection into the flow cell.

Results and Discussion

A. Solution Reaction. 1. Fluorescence Spectroscopy. Figure 1 illustrates a typical emission spectra obtained during a solution reaction at 150 °C (1 wt % in NMP). At time zero (curve 1), hardly any emission is observed, but as the reaction time increases to 30 and 60 min, strong emission is detected. From 120 min and over,

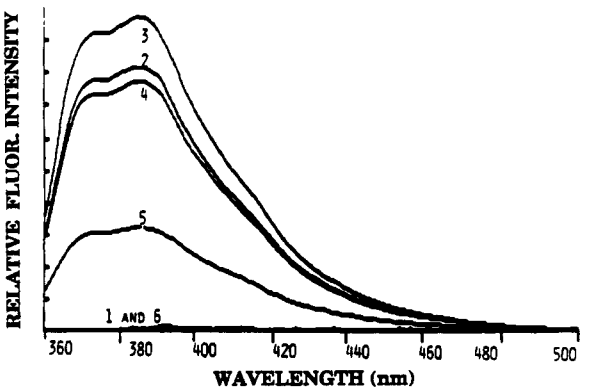

Figure 1. Changes in fluorescence emission spectra during 150 °C solution reaction, as a function of reaction time. Curves 1–6 correspond to reaction times of 0, 30, 60, 120, 240, and 1320 min.

emission decreases, and at 1320 min (curve 6), it has virtually disappeared. Since the preceding paper[1b] on the model compounds clearly indicated that the only significant fluorescent product is the diamine, DAN, and since the observed spectra in Figure 1 resembles that of pure DAN, we interpret the trends observed in Figure 1 as arising from the depolymerized DAN. Therefore, we used the results from Figure 1 to obtain the concentration of depolymerized DAN according to Scheme I. The resulting concentrations of diamine occurring during solution reactions at three temperatures are displayed in Figure 2. We note two trends from Figure 2. First, a maximum of about 9–11% from the DAN moiety in the poly(amic acid) can be initially depolymerized before reacting again. Second, the higher the reaction temperature, the faster the depolymerization with the maximum concentration of DAN increasing with the reaction temperatures. If the amide on both sides of the naphthalene chromophore in poly(amic acid) has to cleave to produce DAN during the reaction, then it is likely that a much larger proportion of cleavages resulting in monoamine species (amine–amic acid or amine–imide) should have occurred at the same time. We can estimate the amount of cleaved monoamine statistically as described in the next section. However, it is important to point out that fluorescence spectroscopy has provided the first direct evidence of depolymerization into monomeric units during solution thermal imidization.

2. Estimate of Chain Cleavage and Molecular Weight Change. If one neglects the substituent effects and assumes equal probability of thermal depolymerization of all amide bonds, it is possible to calculate the total number of depolymerized amide bonds in the following way.[3] Poly(amic acid) can be represented as containing *N* pairs of monomers represented by x (DAN) and y (6FDA) as illustrated:

x–y–x–y–x–y–x–y–x–y–x–y

It can be shown that the expected value of the number of diamine monomers completely depolymerized from poly(amic acid), *X*, can be derived from eq 1,

$$X = n(n+1)/[2(2N-1)] \quad (1)$$

where *n* is the number of the random cleavages. If one solves for *n*, eq 1 can be written as eq 2. Using eq 2, the

$$n = \frac{[1 + 8(2NX - X)]^{1/2} - 1}{2} \quad (2)$$

predicted depolymerized amide bonds can be calculated as in the following example. For a poly(amic acid) with

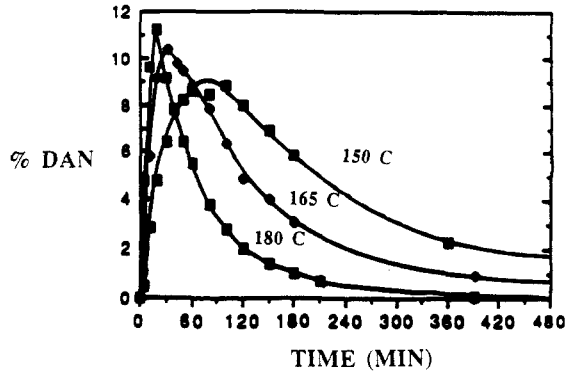

Figure 2. Percentage of depolymerized DAN during solution imidization at 150, 165, and 180 °C via fluorescence spectroscopy.

a molecular weight of 50 000 and a combined molecular weight of x and y of 602.45, N is equal to 83.0. Since ~10% of the DAN moiety in the poly(amic acid) is depolymerized, this corresponds to an X value of 8.30. Substituting these values of N and X in eq 2, the value of n is 51.8. Since 165 amide bonds were originally present on the poly(amic acid), the percentage of the broken amide bonds is 31.4%. Out of 51.8 total amide bond breaks, 16.6 are responsible for the 10% resulting in DAN dissociation. Therefore, 21.4% amide breakage accounts for the percentage of broken bonds which result in non-diamine species. On the basis of the DAN moiety alone, this percentage translates into 42.8%, representing the sum of amic acid–amine and amine–imide.

The effect of 31.4% amide bond dissociation on the molecular weight will be considerable. The reduced number-average molecular weight can be calculated by eq 3, where M_{n_o} is the number-average molecular weight of

$$M_w = M_{n_o}/[(2N-1)f + 1] \quad (3)$$

the original polyamic acid and f is the maximum fraction of depolymerized amide bonds. Using eq 3, an initial molecular weight of 50 000 will be reduced to oligomers with an average molecular weight of 947. A molecular weight reduction of this magnitude is possible, based on the study by Nechayev et al., who reported breakdown into pentamers and trimers.[4]

It should be noted that the predicted amount of depolymerized amide is slightly dependent on the original molecular weight, according to eq 2. For example, for a number-average molecular weight of 5000 which is 10 times smaller than the case described, an experimentally determined diamine concentration of 10 wt % corresponds to 29.6% of the total amide breakage and a reduction in molecular weight to 890. It is reasonable to assume that the initial number-average molecular weight of poly(amic acid) is within the range of 5000–50 000. Therefore, we can conclude that ~30% of the amide bonds have to be cleaved to account for the observed DAN concentration, regardless of the original molecular weight. The comparison between the predicted extent of depolymerization and that actually observed will be tested by size-exclusion chromatography in a later section.

3. UV–Visible Spectroscopy. Although fluorescence spectroscopy is extremely valuable in determining the concentration of diamine during the solution thermal imidizations, it is UV–visible spectroscopy which offers the most information on all the diamine derivatives depicted in Scheme I.

Typical spectra obtained as a function of reaction time are depicted in Figure 3a for constant-concentration al-

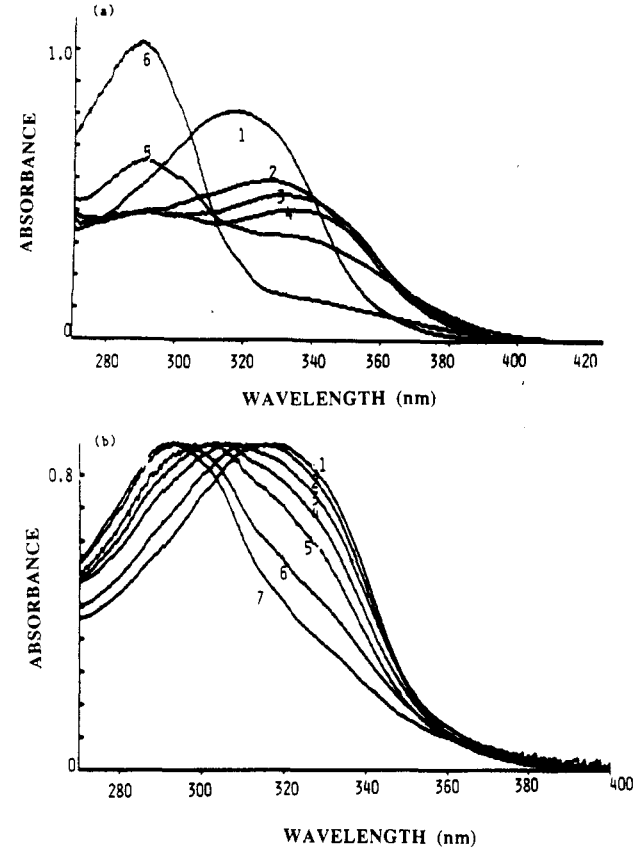

Figure 3. Changes in UV–visible spectra during 150 °C solution reaction (a) and 150 °C solid-state reaction (b). (a) 1–6 correspond to 0, 30, 60, 120, 240, and 1320 min of reaction. (b) 1–7 correspond to 0, 10, 30, 50, 90, 360, and 2160 min of reaction.

iquots. It can be noted in Figure 3a that, early in the reaction, the spectra exhibit a rapid shift of almost 20 nm and a concurrent drop in extinction coefficient. By reference to the UV–visible characteristics of model compounds in the preceding paper,[1b] this trend can be attributed to the conversion of the diamic acid chromophore to amic acid–amine, diamine, and amine–imide as a result of extensive depolymerization. As the reaction further proceeds, the spectra indicate a gradual depletion of the depolymerized species and a simultaneous increase in the concentration of the fully imidized diimide chromophore. It appears, therefore, that the mechanism of imidization and depolymerization suggested by fluorescence results and predicted by Scheme I may be reasonable.

By the deconvolution of UV–visible spectra such as Figure 3a on the basis of the spectra of model species, the composition of all the involved reaction species is obtained as a function of time. Panels a and b of Figure 4 exhibit the composition profile for a 150 °C reaction. It is evident that the rapid depolymerization of poly(amic acid) contributes to a dramatic increase in the concentration of the first depolymerized product, amic acid–amine, to almost 50% (curve 2). The composition of both amic acid–amine and amine–imide obtained by computer fitting exceeds 55%. This compares to ~43% estimated from the statistical model based on the fluorescence results of 10% depolymerized DAN. However, only ~5% depolymerized DAN is detected in UV–visible analysis. The discrepancy between fluorescence and UV–visible results can be explained from at least two different perspectives. One possible explanation is that the substituent effects may play a role in the depolymerization. If the first depolymerization is faster than the second step, then the maximum fraction of amic acid–amine would be expected

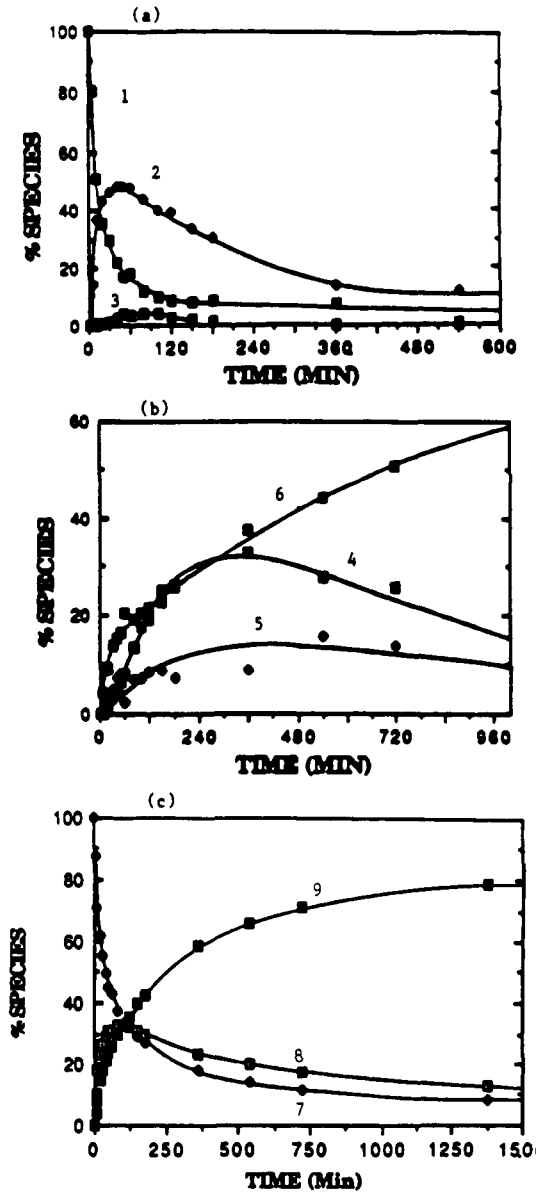

Figure 4. (a, b) Compositional profile of 150 °C solution reaction for (1) diamic acid, (2) amic acid–amine, (3) diamine, (4) amine–imide (5) amic acid–imide, and (6) diimide. (c) Concentration profile of (7) total amide, (8) total amine, and (9) total imide for the same reaction.

Table I
Kinetic Parameters[a] for Solution Thermal Imidization for Poly(amic acid)[b]

temp (°C)	imidizatn rate, K_2[c] ($min^{-1} \times 10^3$)	depolym rate, K_{-1}[c] ($min^{-1} \times 10^3$)	amide formn rate, K_1[c] (L/mol·min × 10^3)
150	5.3	16.0	0.6
165	9.4	32.3	1.1
180	16.5	55.2	1.7
ΔE_a (kcal/mol)	15	16	14

[a] The errors in the rate constants are estimated at most 3%, based on twice the standard deviation values obtained from curve fitting. [b] Poly(amic acid) is made from DAN and 6FDA. [c] See Scheme II for definitions of K_2, K_{-1}, and K_1.

to be greater than that predicted by a random statistical depolymerization process. The enhanced basicity of the amide in the amic acid–amine species as compared to the diamic acid species would support this trend. Another possible explanation is that the close spectral proximity of some of the depolymerized species may distort the calculation of the relative contribution of amic acid–amine,

Scheme II
Polyimide Synthesis Considering Depolymerization

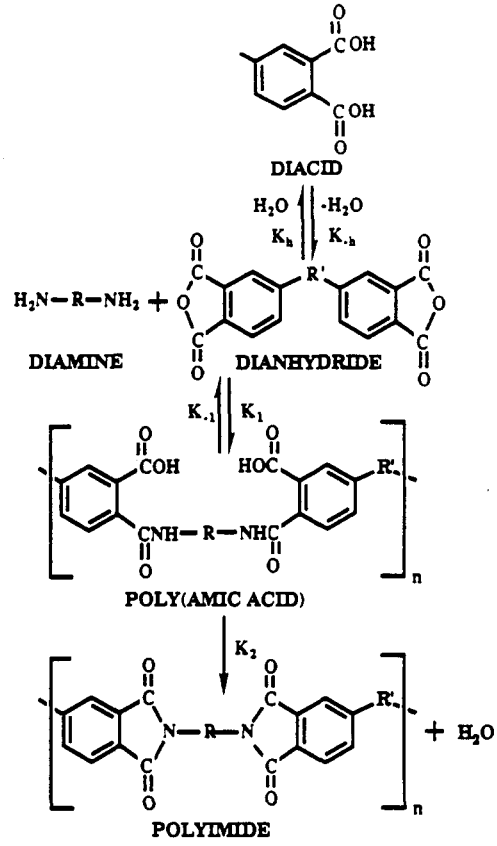

amine–imide, and diamine. For this reason, we believe that the concentration of depolymerized DAN is more accurate by fluorescence than by UV–visible results.

Once compositional analysis is achieved for all six species depicted in Scheme I at three reaction temperatures, the next logical step is to attempt to quantify the rate constants and activation energies for the multitude of reactions indicated in the kinetic scheme. The complicated combinations of the first- and the second-order reactions would be difficult to solve except by extensive computer analysis. Instead, a simplified approach to obtain composite rate constants for the depolymerization rate of the amide (K_{-1}), re-formation of amide (K_1), and imidization (K_2) was made, according to Scheme II, as expressed in eqs 4–6.

$$d[\text{amide}]/dt = K_1[\text{amine}]^2 - (K_{-1} + K_2)[\text{amide}] \quad (4)$$

$$d[\text{amine}]/dt = K_{-1}[\text{amide}] - K_1[\text{amine}]^2 \quad (5)$$

$$d[\text{imide}]/dt = K_2[\text{amide}] \quad (6)$$

The rate constants for these equations can be obtained by multivariable linear regression if values of the differential components could be tabulated. Figure 4c displays a plot of total amide, total amine, and total imide obtained by addition of the previous deconvolution results using six species. The experimental data were fitted with polynomial equations prior to kinetic analysis. Once the d[conc]/dt values were obtained, a multivariable linear regression of these values with respect to the fitted concentrations for eqs 4–6 was performed. The resulting kinetic constants are listed in Table I. The corresponding activation energies are also summarized in Table I.

On the basis of the rate constants listed in Table I, it is clear why depolymerization occurs so rapidly early in the solution reaction. The rate of depolymerization is

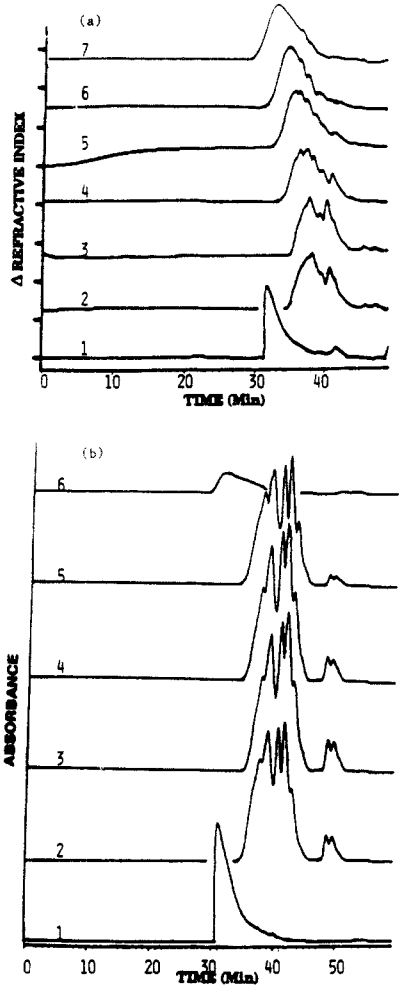

Figure 5. SEC chromatograms for a 150 °C solution reaction via the refractive index detector (a) and via the UV detector set at 345 nm (b). (a) 1–7 correspond to 0, 30, 60, 600, 1320, 1860, and 4200 min of reaction. (b) 1–6 correspond to 0, 30, 60, 120, 240, and 1320 min of reaction.

greater than 3 times the rate of imidization. The later stage of the reaction involves the rate-limiting step of amic acid formation and the relatively rapid rate of imidization.

These results concur with a previous study[5] which demonstrated that the rate-determining step was the slower reaction of amic acid formation. The trend in activation energies also agrees with the few studies reported in the literature.[6] The activation energies of solution imidization and depolymerization of 15 and 16 kcal/mol, respectively, are reasonable when compared to the values of 17 and 22 kcal/mol for different polyimides.[6b]

4. Size-Exclusion Chromatography. Although both fluorescence spectroscopy and UV–visible spectroscopy have provided evidence for a substantial depolymerization reaction which occurs simultaneously with imidization, it would be desirable to have an independent confirmation of a molecular weight reduction of this magnitude. Size-exclusion chromatography (SEC) was chosen to provide this independent confirmation. Figure 5a illustrates the change in SEC chromatograms via the refractive index detector, as a function of solution reaction time. One can qualitatively note that the relatively narrow molecular weight of poly(amic acid) at time 0 (curve 1) rapidly breaks down into distinct oligomeric units early in the reaction before increasing as the reaction proceeds to approach the initial starting molecular weight (curve 7).

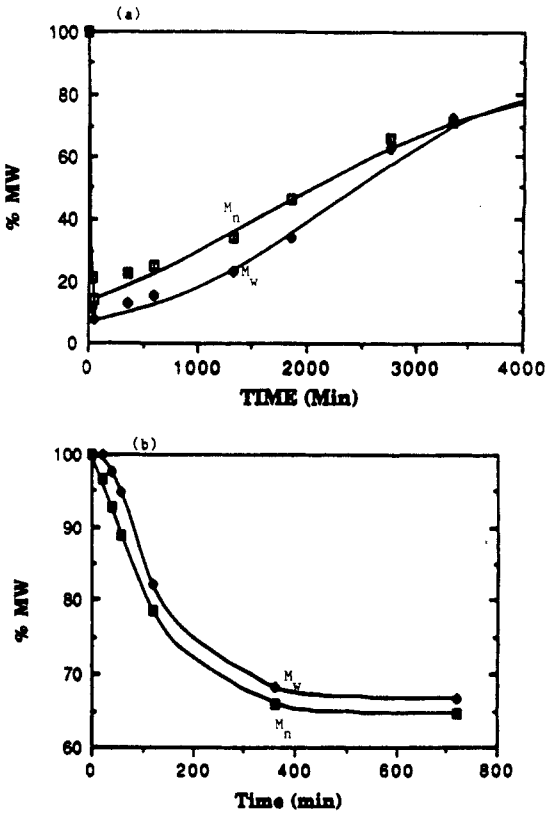

Figure 6. Percent change in number-average and weight-average molecular weight of poly(amic acid) for 150 °C solution reaction (a) and for 150 °C solid-state reaction (b) as a function of reaction time.

No attempt was made to absolutely quantify the extent of depolymerization on the basis of the SEC chromatograms. However, assuming comparable hydrodynamic volume and refractive index for poly(amic acid) and polyimide,[7] we can compare the depolymerization effect on molecular weight relative to a polystyrene standard. The poly(amic acid) number-average and weight-average molecular weights relative to polystyrene change from 5200 and 13 000 to a minimum of approximately 750 and 1000 during the first 120 min of a reaction at 150 °C. The molecular weight gradually increases as the reaction proceeds. Figure 6a presents the change in molecular weight as percentage of the original molecular weight. The large magnitude of the molecular weight decrease in the initial part of the reaction compares well with the prediction set forth by the results of both fluorescence spectroscopy and UV–visible spectroscopy.

If a UV–visible detector is used in conjunction with the refactive index detector, the column resolution is good enought to actually observe the amount of diamine eluting from the SEC column as a peak distinct from that of the NMP solvent. Figure 5b depicts SEC chromatograms for a solution reaction which show the increase and the decrease in DAN concentration near the elution time of 49 min as a function of time. The absence of DAN is observed both at zero reaction time (curve 1) and after extensive reaction time (curve 6). A comparison plot between the concentration of DAN detected by fluorescence spectroscopy and that by SEC is presented in Figure 7. Although the magnitude detected by SEC is somewhat higher than that determined by fluorescence, one can see that the maximum location and the general trend as a function of time is consistent.

Therefore, the use of SEC has provided a considerable amount of information. The magnitude of depolymerization predicted by fluorescence and UV–visible results

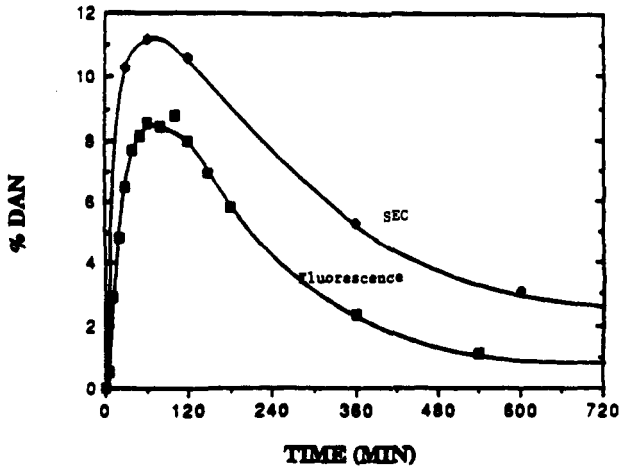

Figure 7. Comparison plot between DAN concentration determined by SEC and by fluorescence spectroscopy for a 150 °C solution reaction.

has been qualitatively observed. The concentration of diamine corresponding to depolymerization has been shown to compare well with that obtained by fluorescence spectroscopy.

5. FTIR Spectroscopy. An independent technique was necessary to check that the compositional change of total imide, total amide, and total amine determined by deconvolution of UV–visible spectra is reasonable. Until now, the possible interconversion of anhydride and diacid has also been ignored to make analysis possible. Infrared spectroscopy is able to supply both the independent confirmation on the composition and the information on interconversion through suitable experimental design.

The out of plane imide bending mode at 722 cm^{-1} was found to be most convenient to monitor the extent of imidization. One of the amide peaks located at 1543 cm^{-1} was used to observe the decrease in amide. The anhydride peak at 1856 cm^{-1} provided information on the extent of interconversion between anhydride and diacid.

Figure 8a displays the observed increase in imidization as a function of increasing reaction time with the NMP solvent substracted from the spectra. While the imide peak increases with reaction time, it is also evident from time zero of Figure 8a that poly(amic acid) has some contribution in this region around 722 cm^{-1}. Due to this limitation, the contribution of amide to the 722-cm^{-1} peak was proportionally subtracted out based on the percent of amide remaining in the solution. Panels b and c of Figures 8 display the decrease in amide concentration and the increase and decrease in anhydride concentration, respectively, during the course of the reaction. The presence of a baseline marred by small depressions is due to water vapor absorbance in the same regions. An attempt was made to interactively correct for this phenomenon as much as possible. However, complete removal of the distortions could not be achieved.

By assuming that the extinction coefficients between the model compound and the naphthalene diimide are reasonably close, the extent of imidization can be quantified and compared to that obtained by UV–visible spectroscopy. For the purpose of quantifying the concentration of amide, the absorbance of poly(amic acid) at time zero was assumed to correspond to 100% amide and subsequent spectra were scaled to this value. In addition to directly comparing the concentration of imide and amide by both FTIR and UV–visible spectroscopy, the combined concentrations of anhydride and diacid, which can be obtained by difference with FTIR, should compare with

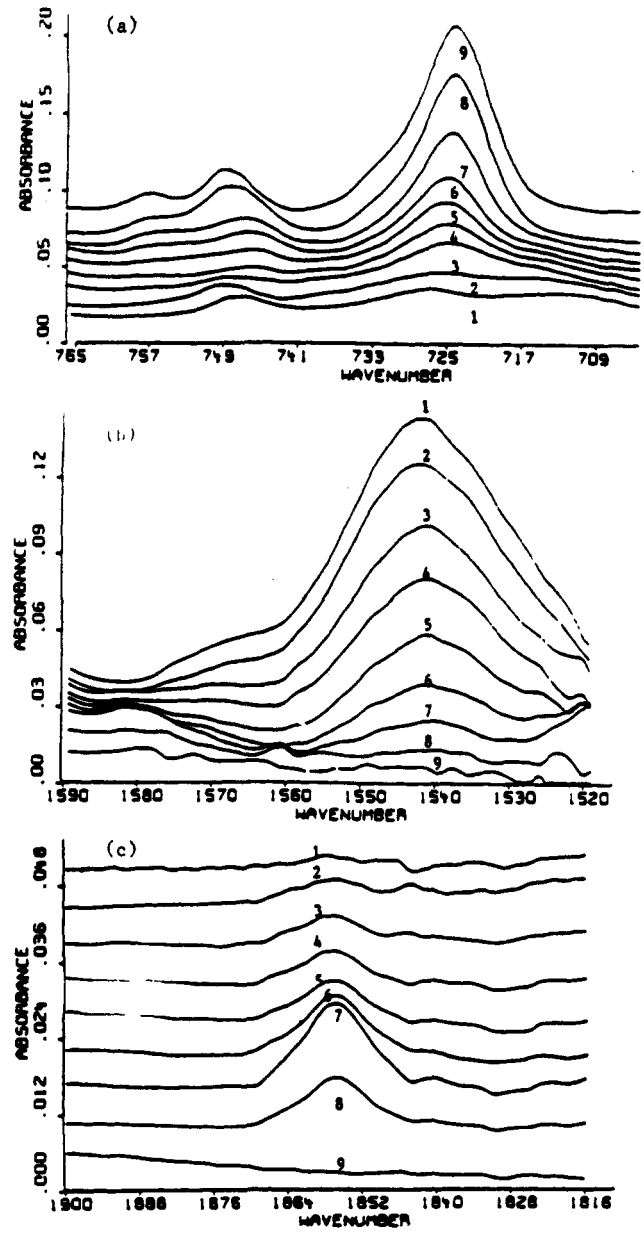

Figure 8. FTIR spectra of (a) 722-cm^{-1} imide peak, (b) 1543-cm^{-1} amide peak, and (c) 1856-cm^{-1} anhydride peak. Curves 1–9 correspond to 0, 5, 20, 35, 65, 120, 360, 1360, and 1950 min of reaction for a 150 °C solution reaction.

the concentration of amine which was obtained by UV–visible spectroscopy.

A comparison between UV–visible and FTIR determination of reaction composition for a 150 °C solution reaction is depicted in Figure 9a–c. Similar results were obtained at 165 and 180 °C. It is evident that comparable results were obtained with the two techniques.

The issue of possible interconversion between anhydride and diacid remains to be investigated. If amide dissociation occurred only due to hydrolysis, one would not anticipate observing the rapid emergence of the anhydride peak early in the reaction as seen in Figure 9. At least one mechanism of depolymerization, therefore, does not result in diacid directly. On the other hand, if the anhydride is stable in solution, the concentration of anhydride present in the reaction should be comparable to that of the concentration of free amine. Figure 10 is a comparison between these two concentrations for a 150 °C reaction, showing that the concentration of anhydride is considerably less than the concentration of free amine during the course of the reaction. This can be interpreted in two

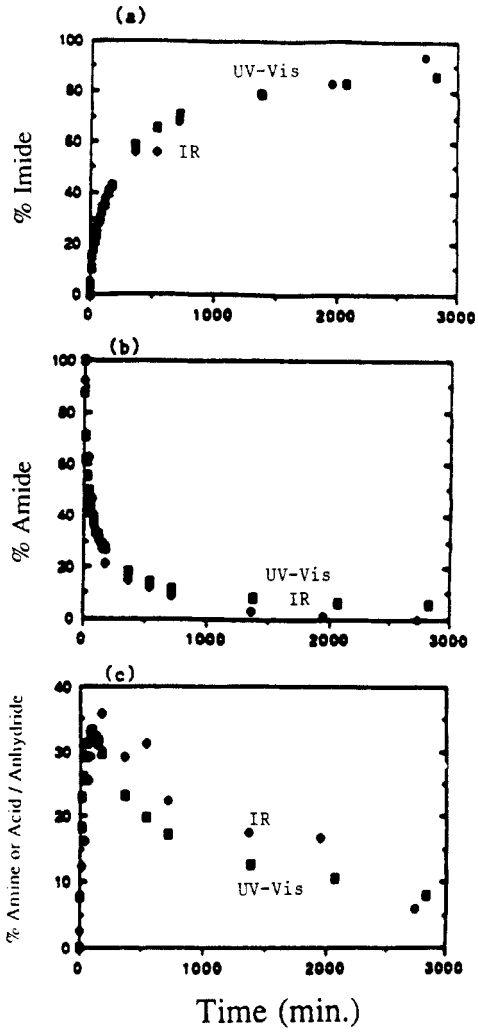

Figure 9. Comparison of (a) imide, (b) amide, and (c) amine–anhydride or diacid concentration by UV-visible and FTIR spectroscopy for a 150 °C solution reaction.

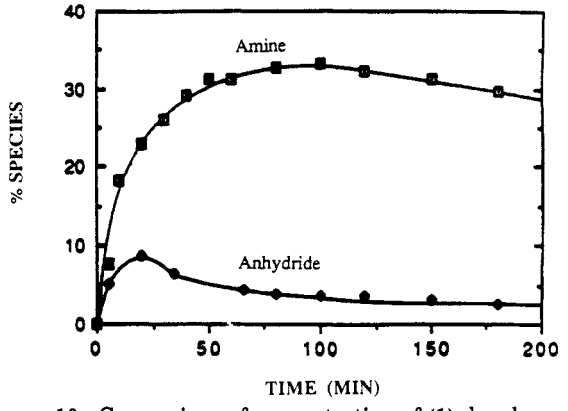

Figure 10. Comparison of concentration of (1) depolymerized amine determined by UV–visible spectroscopy with (2) anhydride concentration determined by FTIR spectroscopy for a 150 °C solution reaction.

ways. One possibility is that there is more than one mode of depolymerization present. It is possible that both thermodynamic depolymerization and amide hydrolysis could be competing processes in the molecular weight reduction. Another possibility is that anhydride is the principal intermediate formed in the depolymerization, but that the presence of condensation product, trace water inherent in the solvent, or basic impurities quickly reacts with the anhydride and reduces its concentration. Clearly, the assumption presented in several dissociation studies[6] that anhydride exists throughout the reaction is invalid. This also explains why similar reaction kinetics were observed when the reaction of a tetracarboxylic acid was compared with a diamine and that of a poly(amic acid). It appears that the formation of amide will be dependent upon the equilibrium between anhydride and diacid. For the purpose of this analysis, the rate of formation of anhydride from diacid or whatever other complex may exist has been incorporated into the rate of amide formation constant.

6. Kinetic Modeling. Although the rate constants and activation energies have been obtained for the solution reactions, some independent confirmation of the validity of these constants was desired. A kinetic simulation program which could synthesize data based on a proposed mechanism and input kinetic parameters would enable comparison between the fit of real data to simulated data. In addition, since only the composite rate constants for imidization, depolymerization, and amide formation have been obtained, a simulation program which could generate all six species of Scheme I would provide information on possible substituent effects.

A kinetic program which has gained popularity since its introduction in 1983, KINSIM,[8] was used for this purpose. As the complexity of a mechanism increases, such as that for Scheme I, the number of terms in the rate expression becomes quite large and it is often mathematically impossible to derive the integrated rate expression. KINSIM is able to simulate kinetic data by internally solving the system of differential equations that apply to a particular mechanism.

Figure 11a is a comparison plot between real data for a 150 °C solution reaction and simulated data using the rate constants listed in Table I and Scheme II. Similar results were obtained for the 165 and 180 °C reactions. Although the simulated spectra deviate slightly from real data later in the reaction, it should be noted that the fit is quite good. Therefore, the rate constants obtained by the previous method are realistic. The deviation later in the reaction might be due to a small extent of oxidation or degradation, although the reaction was conducted under an inert atmosphere.

Since the rate constants presented in Table II have been shown to be realistic, the next step is to simulate Scheme I using the rate constants and compare the results with that of experimental data. The procedure was to substitute the composite rates of imidization listed in Table II into the three unique imidization steps in Scheme I. The same procedure was done for the rates of depolymerization and the rates of amide reformation. If no substituent effects are present, the simulated data should compare reasonably well with that of the experimental data. Figure 11b is a comparison between the simulated and experimental compositions of diamic acid, amic acid–amine, and diamine. It can be seen that the rate of diamic acid depletion and amic acid–amine increase is higher for the experimental data than for the simulated data. It is also evident that the experimental maximum of diamine is lower than that predicted by the simulation. This suggests two possibilities. One is that K_{-1B} is faster and that perhaps K_{1B} is slower than the average dissociation rate. The other is that K_{1A} is faster and that K_{1B} is slower than the average amide re-formation rate. The latter is what potential substituent effects would predict. The basicity of the amide nitrogen on diamic acid should be less than that of amic acid–amine due to the greater electron-donating ability of the free amine group in amic acid–amine. The difference in basicity has been shown to affect the amide formation reaction at low temperatures[9] as previously mentioned, so

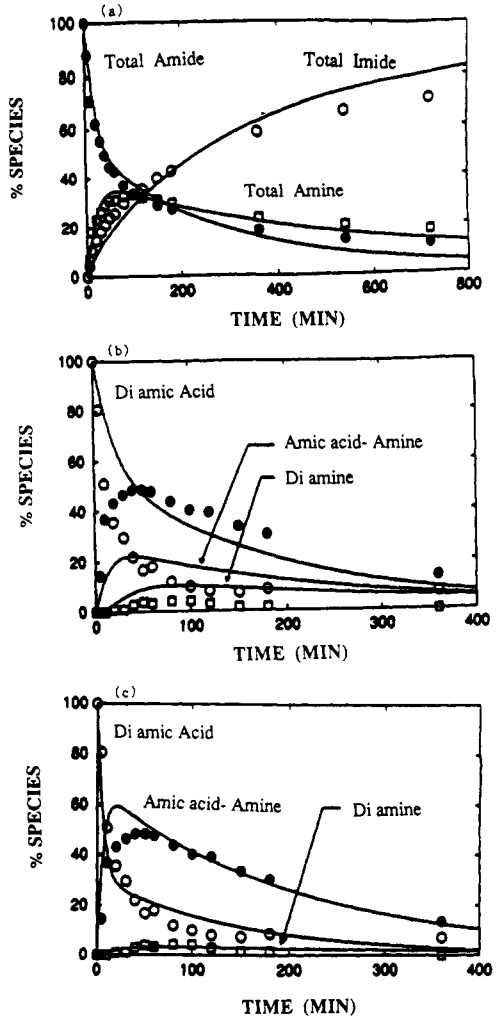

Figure 11. Comparison plot between experimental (data points) and simulated (—) data for a 150 °C solution reaction: (a) for total amine, amide, and imide; (b) for diamic acid, amic acid–amine, and diamine using the rate constants in Table I. For (c), K_{-1B} is 7 times and K_{-1A} is $^1/_6$ that of the composite depolymerization rate constant.

Table II
Kinetic Parameters[a] for Solid-State Thermal Imidization for Poly(amic acid)[b]

	imidization rate ($min^{-1} \times 10^3$)		
temp (°C)	overall, K_2[c]	first, K_{2A}[d]	second, K_{2B}[a]
150	6	6	5
165	14	16	12
180	36	40	30
ΔE_a (kcal/mol)	22	25	23

[a] The errors range from ~2% to a maximum of 10%, based on twice the standard deviation values obtained from curve fitting. [b] Poly(amic acid) made from DAN and 6FDA. [c] See Scheme II for definition of K_2. [d] See Scheme I for definitions of K_{2A} and K_{2B}.

the same effect should also be present at high temperatures.

Since the rate of amide formation is small relative to the rate of depolymerization, however, it suggests that the difference in basicity may also affect the rate of depolymerization. This seems plausible, since the initial decrease in diamic acid should be dominated by this rate. A suggested mechanism for nonhydrolytic depolymerization of amic acid involves competing nucleophilic attack by the hydroxyl oxygen of the carboxylic acid to the amide carbonyl. Any chemical effect which increases the electrophilicity of the amide carbonyl carbon will then increase the rate of depolymerization. It then follows that the less basic nitrogen in the amide of diamic acid could enhance the depolymerization rate by increasing the electrophilicity of the carbonyl carbon relative to that of amic acid–amine.

With this in mind, other simulations were conducted in which K_{-1B} was increased in increments of 100% to that of the composite dissociation rate and K_{-1A} was decreased by the same amount. Figure 11c is another simulation in which all the parameters are the same except that K_{-1B} is 7 times and K_{-1A} is $^1/_6$ that of the composite depolymerization constant. It can be seen that these kinetic constants simulate data which is closer to that of the experimental data. The possibility that amic acid–amine is more stable than the diamine due to either the former or the latter reason correlates with the extent of depolymerization both predicted by fluorescence spectroscopy and confirmed by SEC. A trimer consisting of two amic acid–amine groups connected by the 6FDA moiety would have a molecular weight of approximately 760 for this particular system studied. Since the conjugative effect is not expected to be significant through the fluorinated linkage, a trimer may be the species predicted to be in highest abundance should significant depolymerization occur. The approximate number-average molecular weights obtained at maximum depolymerization support this suggestion. If the dianhydride were fully conjugated, then the electrophilicity of the opposite anhydride groups may depend on whether or not one side has formed an amide linkage and the stability of a trimer would not be as clear cut.

B. Solid-State Reactions. 1. Fluorescence and UV–Visible Spectroscopy. In contrast to the emission spectra obtained during a solution reaction, the emission spectra during a solid-state reaction show no evidence of depolymerized DAN. This result is indicative of the lesser extent of depolymerization in the solid state than in the solution reaction. However, this result does not mean the absence of some random cleavage of the amide bond.

Figure 3b shows typical spectra obtained for a solid-state thermal imidization. In contrast to the solution reactions, it can be noted that only bue shifts occur as a function of time. This can be explained by the lesser degree of depolymerization as compared to the solution reactions. Attempts to deconvolute the spectra based on all six species of Scheme I was unsuccessful due to the small concentration of depolymerized species. It was therefore decided that only the diamic acid, amic acid–imide, and diimide species would be used for the purpose of deconvolution since they are the most abundant. Calculations via SEC information indicate that this contributes less than 5% to the deconvolution error.

A likely explanation for the observed lower rate of solid-state depolymerization may be due to a polymeric cage effect. The concept of a cage effect for imidization has previously been used in an attempt to describe the kinetic slowdown during solid-state reaction.[10] An assumption was made that the cyclization of poly(amic acid) to polyimide requires a correct local orientation in order to occur. The rigidity of the matrix restricts the replenishment of the population of amic acid groups with the correct conformation; thus the reaction slows down upon depletion of the local "cage". A similar concept has been applied to the study of free-radical end groups generated during photooxidation of solid polymers.[11] It was noted that the probability of recombination of generated radicals within the initial cage is often high due to restricted segmental mobility. This same concept can be applied to the resulting end groups upon amic acid depolymerization. The probability of recombination of the anhydride and amine in a

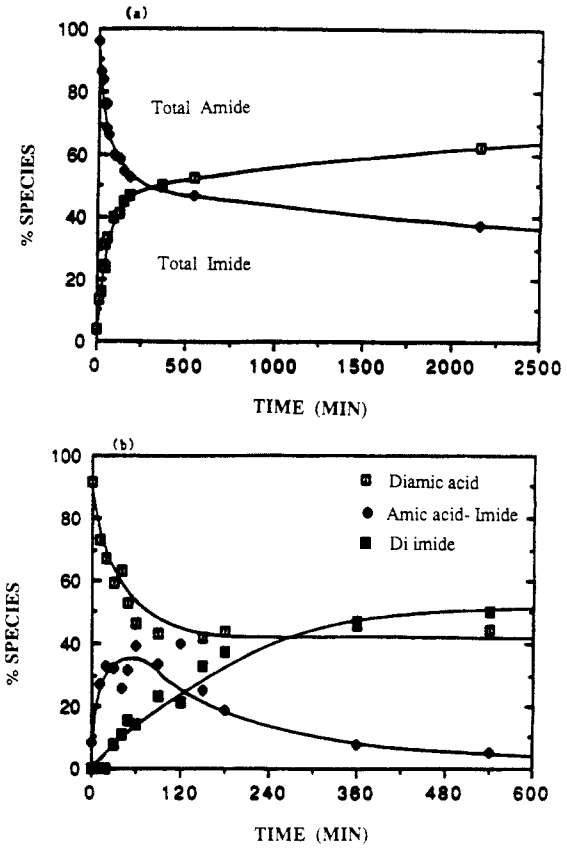

Figure 12. (a) Concentration profile of 150 °C solid-state imidization based on total amide and total imide. (b) Concentration profile of diamic acid, amic acid–imide, and diimide species.

polymeric matrix where local mobility of end groups is restricted should be greater than that of a solution reaction. This cage effect will effectively increase the rate of amide formation from depolymerized end groups, thereby shifting the equilibrium further toward amide stabilization as compared to the solution imidization.

Figure 12a presents the concentration profile of a solid-state imidization based on total amide decrease and total amide increase. The kinetic slowdown mentioned in the literature is also evident with these reactions, as noted by the sudden decrease in imidization rate between 40 and 50% conversion. The total compositional profile of the same reaction is depicted in Figure 12b. As expected, the amic acid–imide can be observed as an intermediate which reaches a maximum and then decreases upon further conversion to diimide.

The analytical approach used to obtain rate constants for the solution imidization reactions can also be applied to the solid-state reactions. Since solvent loss and possible vitrification results in a decrease in rate constant as the reaction proceeds, only the initial portions of the composition were used to determine rate constants. For the 150, 165, and 180 °C reactions, the first 60, 40, and 20 min were used, respectively. Table II lists the kinetic constants and the activation energies.

The constant K_2 is the rate of imidization determined from regression of the data of the type presented in Figure 12a. The validity of these kinetic parameters will be demonstrated in the section on kinetic simulation.

The first item worth noting from Table II is that although the activation energies for solid-state imidization are typical for previously mentioned solid systems, they are slightly higher than that for the solution reactions. This seems plausible since cyclization in the solid state may experience difficulties which do not occur in solution. There may be steric hindrance caused by the close proximity of neighboring polymers. An increase in temperature for the solid state should enhance the mobility of the polymer to a greater degree than that for solution. The decomplexation of solvent may also contribute to the higher activation energy. Since it was previously mentioned that decomplexation of solvent is required prior to imidization,[12] perhaps this is a rate-limiting step which in itself has a high activation energy.

Comparison of the rate of the first ring closure of diamic acid to that of the second ring closure of amic acid–amine was anticipated to yield information on possible substituent effects. On the basis of the data for K_{2A} and K_{2B} at each respective temperature, it appears that a subtle substituent effect may be present but that, in general, the rates are well within a factor of 2 of each other. As expected, the rate of diamic acid conversion to amic acid–imide should be faster than the rate of reaction from amic acid–imide to diimide due to the greater withdrawing effect of the imide as compared to the amide.[1] Since the activation energies for both rates are reasonably close, no inferences should be drawn about the subtle deviation.

2. Size-Exclusion Chromatography. Although the absence of red shifts in the UV–visible spectra for a solid-state reaction suggests that the depolymerization reaction is minor, the effect on molecular weight of even a small extent of depolymerization should be detectable by SEC. Figure 6b illustrates the percent decrease in molecular weight which occurs during an isothermal solid-state reaction relative to the polystyrene calibration plot. When Figure 6b is compared with Figure 6a, it can be seen that both the rate and extent of depolymerization is appreciably less for the solid than for the solution. Regardless, an approximately 30% reduction in molecular weight does occur during the solid-state reaction. This is actually less than the 70% minimum in M_n reported by Young et al. for another soluble polyimide film.[13]

It is also evident that the molecular weight does not increase later in the reaction comparison to the solution reactions. This is most likely due to the decreasing mobility as the solvent and condensation product are volatized and the extent of imidization increases. If the reaction were not isothermal, but ramped in temperature as is commonly done in industry, greater mobility at higher temperatures will allow a percentage of the depolymerized end groups to imidize. For the experiment illustrated in Figure 6b, the temperature was later increased to 280 °C for 1 h to examine the effect on molecular weight. The number-average molecular weight increased to 7800 and the weight-average molecular weight increased to 18 100, which are respectively 72 and 89% of the original poly(amic acid) molecular weight.

3. FTIR Spectroscopy. Infrared spectroscopic analysis was able to confirm that the compositional profile determined by UV–visible spectroscopy for solution reaction was reasonable. In order to provide a similar confirmation for solid-state reactions, we monitored the extent of imidization in solid films by using the 722-cm^{-1} imide peak calibrated with the 1209-cm^{-1} peak for a carbon–fluorine stretching band as an internal standard. A solid sample which was reacted at 290 °C for ~1 h was used as the fully imidized reference by which all other samples were scaled. Figure 13 is a comparison between the extent of imidization determined by both UV–visible deconvolution and FTIR. It can be seen that the two techniques compare quite well.

4. Kinetic Modeling. Kinetic modeling of the solution reactions using rate constants obtained by linear regression

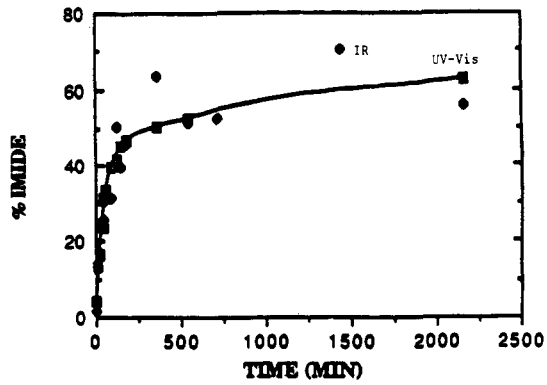

Figure 13. Comparison of imide concentration for a 150 °C solid-state reaction determined by both UV–visible and FTIR spectroscopy.

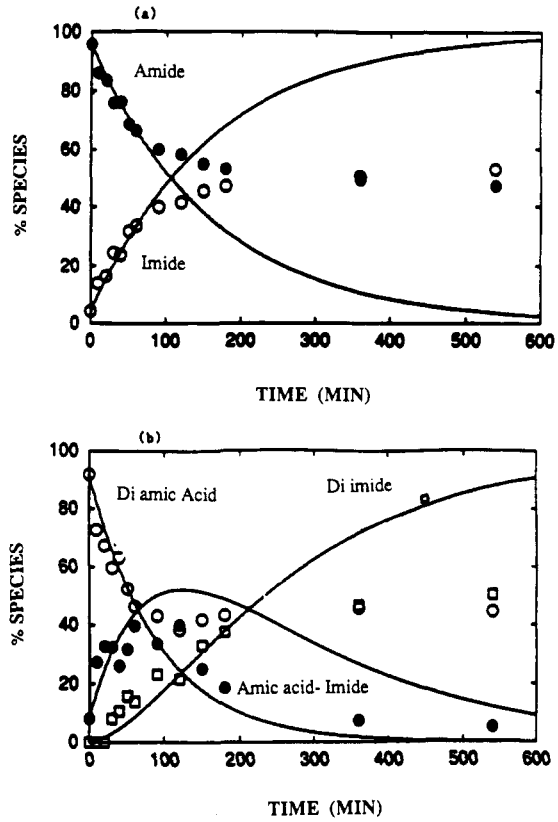

Figure 14. Comparison plot between experimental (data points) and simulated (—) data for a 150 °C solid-state reaction for total amide and imide (a) and for diamic acid, amic acid–imide, and diimide (b).

was demonstrated to yield reasonable comparisons to experimental data when composite concentrations of amide, imide, and amine were considered. In the same manner, it was decided that a simulation of solid-state UV–visible deconvolution data using the rate constants in Table II would be valuable. For the solid-state reactions, however, the simulated data would only be expected to favorably compare with experimental data during the early time of the reactions. Within less than 1 h at 150 °C, the reduced mobility of the reaction medium has been shown to slow the reaction considerably.

Figure 14a is a comparison plot between experimental data considering total amide and total imide for a solid-state reaction and the simulated data using the K_T rate constants presented in Table II. It can be noted that the fit is quite good until approximately 40% conversion to imide, where the experimental rate constants are seen to slow down and the simulated data continue to completion. The difference between the two plots shows the dramatic effect that the matrix has upon the solid-state reaction.

A comparison between the experimental deconvolution data for diamic acid, amic acid–imide, and diimide species and those from the simulated data using the rate constants from Table II is depicted in Figure 14b. Again the fit is quite good until the matrix effects slow the reaction rate.

Summary

The use of 1,5-diaminonaphthalene to investigate thermal imidization both in the solution and in the solid state has been a rewarding endeavor. Although all goals originally set could not be realized, a considerable amount of information was obtained. The initial intent of extrapolating information obtained for the solution reactions to that of the solid-state reactions was achieved.

Through characterization of the solution reactions, the commonly reported viscosity decrease during high-temperature poly(amic acid) aging or imidization can be understood to be a result of a competing depolymerization. The rate constant of depolymerization was actually determined to be greater than the rate constant of imidization for this particular system, explaining the rapid initial depolymerization. For the first time, initial depolymerization to monomeric diamine was confirmed. The rate of formation of amic acid was determined to be the rate-limiting step in the gradual conversion of the depolymerized species into resulting polyimide.

In contrast to data presented in several previously mentioned studies, there did not appear to be an appreciable change in the rate constants during the entire course of the solution reaction. Any deviation in the extent of imidization late in the reaction may be a result of water azeotroping with the highly hygroscopic reaction solvent or trace amine oxidation. Perhaps some literature reports of a solution kinetic slowdown are due to the competing dissociation reaction which has not been taken into account. Also, contrary to other previously mentioned depolymerization studies, anhydride was found not to be a stable dissociated species during the reaction. In fact, the conversion of anhydride to diacid may contribute to the experimentally determined slow rate of amide reformation. Attempts to simulate all six species based on Scheme I lead to the conclusion that electron density differences on the nitrogen as a result of substituent effects seem to result in a difference in the depolymerization equilibrium between some species. The apparently faster rate of depolymerization to amic acid–amine was compared to diamine supports this assumption. Due to the complexity of Scheme I, however, the quantitative analysis of all rate constants was not possible.

The solid-state reactions also led to some interesting results. The extent of depolymerization is much less than that during the solution reaction. The activation enegy of imidization was found to be greater than that of solution imidization, perhaps due to mobility constraints present even early in the reaction or to solvent decomplexation phenomena. The presence of substituent effects during imidization was noted, but the effects seem to be less dramatic than that of depolymerization or amide reformation. Although imidization autocatalysis by adjacent carboxylic acid groups may exist, direct confirmation was not possible due to the dominant limitations on matrix mobility after a brief period of time. Size-exclusion chromatography demonstrated that although less of a depolymerization reaction occurs in the solid state as compared to solution, the reaction was still present. The extent of depolymerization was reasonable as compared to the only

other SEC film depolymerization study.[13] Possible explanations for the decrease in depolymerization include an amide equilibrium constant which favors amide formation due to a polymeric cage effect and greater anhydride stability. The matrix mobility, as mentioned in many other published works, again appeared to be a major factor in decreasing the imidization rate after only short reaction times. Modeling studies were able to illustrate the dramatic slowdown in imidization rate.

Acknowledgment. We acknowledge financial support of this work by the National Science Foundation (Grant DMR 8703908), the Army Research Office (Contract DAA L03-89-k-0081), and NASA (Grant NAG-1-931). P.R.D. is grateful for the Connecticut High Technology Fellowship support. We are also grateful for helpful discussions and encouragement by Drs. P. Young and T. St. Clair of NASA.

References and Notes

(1) (a) Pyun, E.; Mathisen, R. J.; Sung, C. S. P. *Macromolecules* **1989**, *22*, 1174. (b) Kailani, M. H.; Sung, C. S. P.; Huang, S. J. *Macromolecules*, preceding paper in this issue.

(2) (a) Dine-Hart, R. A.; Wright, W. W. *Makromol. Chem.* **1971**, *143*, 189. (b) Kotov, B. V.; Gordina, T. A.; Voischchev, V. S.; Kalninov, O. V.; Pravednikov, A. N. *Vysokomol. Soedin.* **1977**, *A19*, 614.

(3) We acknowledge the kind help on the statistical approach from Prof. U. Koehn, Statistics Department, University of Connecticut, 1990.

(4) Nechayev, P. P.; Vygodskii, Y. S.; Zaikov, Y. E.; Vinogradova, S. V. *Polym. Sci. USSR* **1976**, *A18* (8), 1903.

(5) Gerashchenko, Z. V.; Vygodskii, Y. S.; Slonimskii, G. L.; Askadskii, A. A.; Papkov, V. S.; Vinogradova, S. V.; Dashevskii, V. G.; Klimova, V. A.; Sherman, F. B.; Korshak, V. V. *Polym. Sci. USSR*, **1973**, *A15* (8), 1927.

(6) (a) Kamzolkina, Y. E.; Teiyes, G.; Nechayev, P. P.; Geraschenko, Z. V.; Vygodskii, Y. S.; Zaikov, G. Y. *Polym. Sci. USSR* **1976**, *A18* (12), 3161. (b) Kamzolkina, E. V.; Nechaev, P. P.; Markin, U. S.; Vygodskii, Y. S.; Grigoreva, T. V.; Zaikov, G. E. *Dokl. Akad.* **1974**, *219* (3), 1105.

(7) Baranovskaya, I. A.; Kudryavtsev, V. V.; Dyakonova, N. V.; Sklizkova, V. P.; Eskin, V. Y.; Koton, M. M. *Polym. Sci. USSR* **1985**, *A27* (3), 677.

(8) Barshop, B. A.; Wrenn, R. F.; Frieden, C. *Anal. Biochem.* **1983**, *130*, 134.

(9) Koton, M. M. *Polym. Sci. USSR* **1971**, *A13* (6), 1513.

(10) Bessonov, M. I.; Koton, M. M.; Kudryavtsev; Laius, L. A. *Polyimides: Thermally Stable Polymers*; Plenum: New York, 1987.

(11) Garton, A.; Carlsson, D. J.; Wiles, D. M. *Makromol. Chem.* **1980**, *181*, 1841.

(12) Brekner, M. J.; Feger, C. *J. Polym. Sci., Polym. Chem.* **1987**, *25*, 2479.

(13) Young, P. R.; Davis, J. R.; Chang, A. C.; Richardson, J. N. *J. Polym. Sci., Polym. Chem.* **1990**, *28*, 3107.